

Available online at www.sciencedirect.com**ScienceDirect**

Energy Procedia 94 (2016) 241 – 248

Energy

Procedia

13th Deep Sea Offshore Wind R&D Conference, EERA DeepWind'2016, 20-22 January 2016,
Trondheim, Norway

Adaptation of Controller Concepts for Support Structure Load Mitigation of Offshore Wind Turbines

Binita Shrestha*, Martin Kühn

ForWind, Wind Energy Systems, University of Oldenburg, Ammerländer Herrstrasse 136, 26129 Oldenburg, Germany

Abstract

Different controller concepts can be employed for the support structure load reduction of offshore wind turbines, however, they entail unfavorable collateral effects like additional actuator wear or load fluctuations in other turbine components. Hence, there is a need to identify possibilities of employing such controller concepts only under particular loading and operational conditions e.g. sea states with high waves or large wind-wave misalignment when their load reduction potential is high in relation to their unfavorable side effects. This paper introduces a multi-objective optimization method to perform a trade-off analysis between the reduction of damage equivalent fatigue loads at the monopile support structure and the collateral effects of the different controller concepts. The optimization is performed considering the baseline controller, plus tower fore-aft controller to reduce the tower fore-aft bending moment and the active generator torque controller to reduce the side-to-side load. These two concepts increase the pitch activity and drive train torque variability as collateral effect, respectively. With the optimization methodology presented, it is possible to identify the most efficient operation time to activate different control concepts under each load case, utilizing their advantageous load reduction while limiting their penalty in collateral effects.

© 2016 The Authors. Published by Elsevier Ltd. This is an open access article under the CC BY-NC-ND license

(<http://creativecommons.org/licenses/by-nc-nd/4.0/>).

Peer-review under responsibility of SINTEF Energi AS

Keywords: Support structure load; controller collateral effects; offshore wind turbine; trade-off analysis; multi-objective optimization

1. Introduction

Support structures can account for more than 36 % of offshore wind farm costs [1], partially due to the aerodynamic and hydrodynamic loads produced by the offshore environmental conditions. There are several active control concepts available for load mitigation [2][3][4] in the wind industry, which can reduce effectively the loads in the support structure, while encountering collateral effects of higher loads in other components of the turbine. As a consequence the wind turbine lifetime could be reduced and an increase in unscheduled maintenance might occur. While the potential for reducing support structure loads due to the implementation of different load mitigation concepts has been already analyzed by several researches [4][5][6], Fischer presented a methodology to employ certain controller concepts at particular loading and operational conditions [7]. Furthermore, Fischer evaluated, at least qualitatively, the

* Corresponding author. Tel.: +49-441-798-5063 ; fax: +49-441-798-5099.

E-mail address: binita.shrestha@forwind.de

	Support structure		Rotor-nacelle assembly					Additional ULS check	Energy yield	Power fluctuations	System costs
	Fore-aft	Side-to-side	Blades	Hub	Yaw	Gearbox	Pitch drives				
Tower Feedback Control	↓	→	↗	↗	↗	↗	↗		→	→	→
Active Idling Control	↘	→	↗	↗	↗	↗	↗	●	→	→	→
Individual Pitch Control	↗	↓	↗	↘	↘	→	↑	●	→	→	→
Active Generator Torque Control	→	↓	→	↓	↘	↗	→		→	↑	→
Soft cut-out	↓	↗	↗	↗	↗	↗	↗	●	↑	↗	→
Semi-active mass damper	↓	↓	→	→	→	→	→	●	→	→	↑

Fig. 1. Qualitative fatigue load influences of dynamic control concepts [7].

collateral effects of certain load mitigation concepts on other turbine components, which is illustrated in Fig. 1. Firstly, it can be seen that while quantifying the load reduction at a particular hot spot is straight forward, the evaluation and judgement of the various collateral effects inside the whole turbine system is a rather complex task. Secondly, for the reduction of certain load components, e.g. support structure side-to-side response, more than one option might be available, such as individual pitch control and active generator torque control. However, the collateral effects of such concepts could be quite different, both in magnitude and where they occur within the turbine system.

Few research [8] has been performed to implement the controller concepts not only to reduce the support structure loads but also to limit the collateral effects in a more rational manner. The objective of this paper is to introduce a methodology to approach the trade-off analysis between the reduction of damage equivalent fatigue loads in the support structure and the collateral effects due to the employment of different controller concepts at an exemplified and simplified reference case. A multi-objective optimization method is introduced and performed for the controller activation, considering tower fore-aft controller (TFA) to reduce the tower fore-aft load and active generator torque controller (AGT) to reduce the side-to-side load. The collateral effects considered are increase in pitch activity and drive train torque variability, respectively. Such a multi-objective optimization is regarded as a key element of a more comprehensive system for adaptive operational control, where both sea state conditions and turbine load response is monitored online in order to select the most effective load mitigation controller concepts with respect to a trade-off between load reduction and collateral effects. A brief outline of such a system is discussed in Section 4.

2. Methodology

The hydro-servo-aeroelastic simulation is performed for the 5 MW UpWind [9] turbine on a monopile support structure with the first tower eigen frequency of 0.28 Hz. In this section, the environmental conditions, controllers and other parameters selected are briefly described, and finally the methodology for the trade-off study is explained.

2.1. Environmental condition and sea state lumping

The numerical simulation is set with reference to the external conditions derived from the K13 met-mast located in the Dutch North Sea at 25 m water depth (MSL) [10]. The high hydrodynamic excitation of the relatively soft monopile support structure at deep water locations can be quite sensitive to the wind and wave misalignment. This is because the high aerodynamic damping during the power production mode is acting only in the fore-aft rather than the side-to-side direction. Hence, up to 30° wind-wave misalignment, the loading on the monopile at the seabed can be maximum in the fore-aft direction while the higher loads can occur in the sideways direction for larger misalignment [7][11]. Because of this effect, sea states with different wind-wave misalignments are considered in this exemplary investigation. Meanwhile, only one mean wind speed of 14 m/s with 14.4 % turbulence intensity is taken into account, while the full operating range of the wind speed would be considered in the future extension of this research. Four

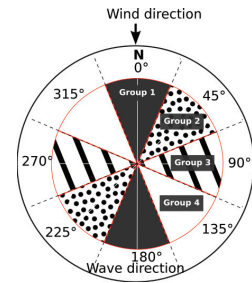


Fig. 2. Wind-wave misalignment groups, with wind coming from the North. The groups are formed merging opposite wind and wave directions.

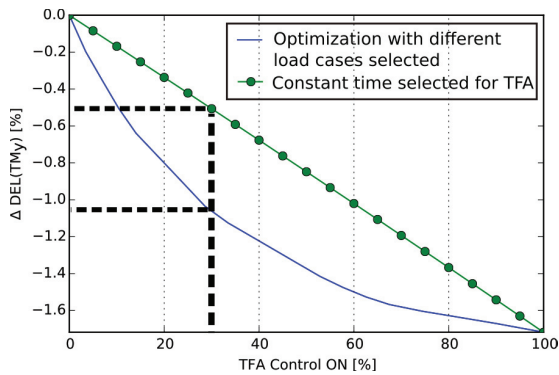


Fig. 3. Fore-aft load reduction with and without the optimization.

different wind-wave misalignment groups of 0° , 45° , 90° and 135° are considered with wind coming always from the North and using 45° wave direction bins. As shown in Fig. 2, the misalignment groups are done merging with the opposite direction. In order to limit the computational effort to a reasonable amount, the number of sea states is reduced by a so-called sea state lumping. Each lumped sea state is further represented by a certain significant wave height and wave peak period calculated according to [11]. The chosen 14 load cases are listed in Table 1.

2.2. Load simulations

The three dimensional turbulent wind field with a Kaimal model and irregular sea states according to the Pierson-Moskowitz spectrum is used for the hydro-servo-aeroelastic simulations which are performed using GH Bladed v4.4 [12]. The Design Load Case 1.2 according to [13] is selected to analyse fatigue loads during the power production. Six random wind seeds with 10 minutes duration are employed. The damage equivalent loads of the bending moment in fore-aft and side-to-side directions at the mudline location are calculated using the rainflow cycle counting method, considering a reference cycle number of $2E7$ for 20 years lifetime and an inverse S-N-slope of 4, typical for steel.

2.3. Control concepts

The scope of this paper is to optimize the usage of the controllers with respect to the trade-off analysis rather than to optimize different controllers itself. Therefore, the magnitude of the actual load reduction achieved by certain controllers in this paper is indicative. The following three control concepts are chosen:

- Baseline controller (BLC): The power production operation employs the generator-torque controller to maximize the power in the below-rated region and the blade-pitch controller to regulate generator speed in the rated power region. The controller is based on [14] with the correction of gain scheduling according to [15].
- Tower fore-aft controller (TFA): TFA is based on the UpWind controller [9]. An additional pitch angle is determined using the tower fore-aft acceleration and is superimposed to the pitch angle provided by the BLC. This is done in order to enhance the aerodynamic damping and hence to reduce the tower fore-aft displacement. The collateral effect is an increase in the pitch activity, which is represented here by the pitch Actuator Duty Cycle [16] and is defined as:

$$ADC = \sum_i (p_i \cdot ADC_i) = \sum_i (p_i \cdot \frac{1}{T} \int_0^T \frac{\dot{\beta}(t,i)}{\dot{\beta}_{norm}} dt) ; \dot{\beta}_{norm} = \begin{cases} \dot{\beta}_{max} , & \dot{\beta}(t,i) \geq 0 \\ \dot{\beta}_{min} , & \dot{\beta}(t,i) < 0 \end{cases} \quad (1)$$

Table 1. Lumped load cases (wind speed of 14 m/s) and their actual observed frequency at K13 Location.

Wind-wave misalignment[$^\circ$]	Significant wave height[m]	Peak period [s]	Probability [-]
0	0.9	5.0	0.00249
0	1.5	6.0	0.00266
0	2.4	6.9	0.00210
45	0.5	4.7	0.00039
45	1.0	5.2	0.00081
45	1.5	6.0	0.00084
45	2.4	6.8	0.00092
90	1.0	5.3	0.00020
90	1.5	6.1	0.00012
90	2.5	7.0	0.00025
135	0.8	4.9	0.00050
135	1.5	6.0	0.00036
135	2.0	6.8	0.00037
135	3.0	7.7	0.00040

where, p_i : probability of occurrence of a particular sea state i of duration T (here 10 minutes)
 $\dot{\beta}$: time series of the blade pitch rate [m/s]
 $\dot{\beta}_{norm}$: the maximum or the minimum allowable pitch rate

- c. Active generator torque controller (AGT): The AGT uses the tower side-to-side acceleration to determine an additional tower side-to-side damping torque and is superimposed to the generator torque provided by the BLC. The penalty of implementing AGT are higher fluctuations in drive train and power electronics [7]. For the trade-off analysis, the standard deviation of the generator torque is considered as the collateral effect.

2.4. Trade-off analysis approach: Multi-objective optimization

A multi-objective optimization approach is proposed to activate the 'most effective' controller for the given sea state conditions to perform the trade-off between minimizing both the support structure loads and the collateral effects simultaneously. In this section, the optimization criteria used for the three controller sets will be described.

- a. Tailoring the tower fore-aft controller (TFA) versus the baseline controller (BLC)

Instead of operating TFA controller for 100 % of time, an optimization analysis is performed with the objective to minimize the tower fore-aft damage equivalent load while limiting the collateral effect, i.e. pitch Actuator Duty Cycle (ADC). The linear optimization performed using a Python script [17] gives the optimal percentage of time that the TFA controller should be activated, $q_{2,i}$, or when only BLC should be operated, $q_{1,i}$ for each load case i , where, $q_{2,i} + q_{1,i} = 1$. A maximum allowable pitch ADC value is defined with a constraint factor, C_{ADC} , expressed as percentage of the increase in pitch ADC when TFA is fully activated. The optimization criteria is to limit the final pitch ADC value to the maximum allowable pitch ADC. That is, for the given C_{ADC} , the constraint equation for the optimization is defined as:

$$\begin{aligned} ADC_{final} &\leq ADC_{max}; \\ ADC_{final} &= \sum_i (ADC_{BLC,i} \cdot q_{1,i} + ADC_{TFA,i} \cdot q_{2,i}); \\ ADC_{max} &= \sum_i (ADC_{BLC,i} + C_{ADC} (ADC_{TFA,i} - ADC_{BLC,i})) \end{aligned} \quad (2)$$

where,

C_{ADC} : constraint factor, $0 \leq C_{ADC} \leq 1$
 ADC_{BLC} : pitch ADC when only BLC is operating
 ADC_{TFA} : pitch ADC when activating TFA for 100 % time

The objective of the optimization is to minimize the damage equivalent load given by:

$$DEL(TM_y) = \sqrt{\sum_i p_i \cdot (q_{1,i} \cdot DEL(TM_y)_{BLC,i}^m + q_{2,i} \cdot DEL(TM_y)_{TFA,i}^m)} \quad (3)$$

where,

m : inverse slope of S-N curve (here 4, typical for steel)
 p_i : probability of occurrence of a particular sea state i
 $DEL(TM_y)_{BLC}$: tower fore-aft DEL at mudline when only BLC is activated
 $DEL(TM_y)_{TFA}$: tower fore-aft DEL at mudline when TFA is fully activated

- b. Tailoring the active generator torque control (AGT) versus the baseline controller (BLC)

The second multi-objective optimization is used for AGT and BLC controllers to minimize the tower side-to-side damage equivalent load ($DEL(TM_x)$), limiting its collateral effect, i.e. standard deviation of the generator torque. The result of the optimization likewise to Eq. 2 and 3 gives the optimal percentage of time that the AGT controller should operate during each load case.

- c. Tailoring the tower fore-aft (TFA) and active generator torque (AGT) versus the baseline controller (BLC)

In order to take advantage of different load mitigation concepts, different controllers could be considered at the same time. The multi-objective optimization is carried out for TFA, AGT and BLC controllers with the objective of minimizing $DEL(TM_{xy})$, which is the time series of the resultant vector of the tower fore-aft and side-to-side loads, limiting the collateral effect from both controllers, i.e. pitch ADC and standard deviation of generator torque. In the present case, the optimization is performed under different maximum allowable pitch ADC and

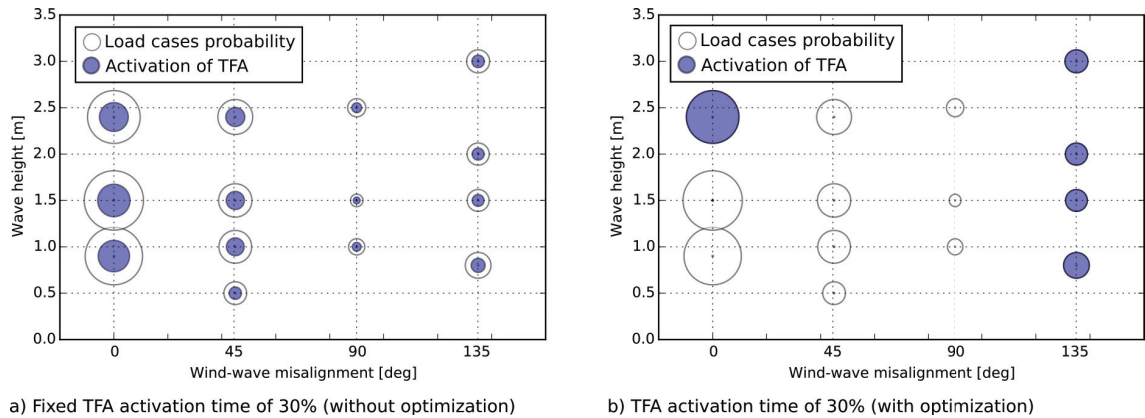


Fig. 4. Load cases scatter diagram of significant wave height and wind-wave misalignment a) without and b) with optimized controller activation for 30 % of the total time. The outer circle area represents the total probability and the colored circle area the proportion when TFA is activated.

standard deviation of generator torque values, and the range is defined by the change in pitch ADC and standard deviation of generator torque while activating 100 % of the time BLC or the controller TFA and AGT respectively. For the sake of simplicity, the same constraint factor for both the pitch ADC and standard deviation of generator torque is considered and both the TFA and AGT controllers are activated simultaneously.

2.5. Illustration of optimization effect on load case selection

In order to check if it is necessary to perform the optimization for each load case, or if the same objective, i.e. to minimize the damage equivalent load and limit the increase in collateral effect, could be reached activating the controller for a determined time, a preliminary analysis is performed with BLC and TFA controllers for the 14 load cases listed in Table 1. For this analysis, the TFA controller is activated independently from the sea state conditions for a fixed percentage of time without optimization. Secondly, the multi-objective optimization, described in Section 2.4, is performed to find the optimal TFA operation time for each load case in order to minimize the tower fore-aft damage equivalent load, $DEL(TM_y)$, calculated at mudline location (Eq. 3) constrained on the pitch ADC given in Eq. 2 with C_{ADC} ranging from 0 to 1.

Fig. 3 illustrates the reduced $DEL(TM_y)$ for the case without optimization in green marked curve and with optimization in blue. The difference between the two curves represents the added advantage of the optimization. For example, let us consider when TFA is activated 30 % of the total time, represented with dotted lines in Fig. 3. For the case without optimization, the $DEL(TM_y)$ is reduced by 0.51 %, which corresponds to 29.5 % of the maximum achievable load reduction with the TFA controller. Here, the $DEL(TM_y)$ is calculated using Eq. 3 with $q_{2,i} = 0.3$ for all load cases i . Whereas, for the optimized case, the optimization performed to minimize the $DEL(TM_y)$ in Eq. 3 with different ADC constraint in Eq. 2 gives the optimal operation time of TFA for each load case, $q_{2,i}$. When the optimization resulted in 30 % TFA activation time, the $DEL(TM_y)$ is reduced by 1.08 %, equivalent to 62 % of the maximum achievable load reduction. Meanwhile, the resulting pitch ADC for the cases with and without optimization is increased by 36.5 % and 30 % of the pitch ADC for a continuous TFA employment, respectively. These results confirm that optimizing the controller activation time for each load case can yield higher load reduction with significantly lower increase of the collateral effect compared to controller activation ignoring the actual sea state conditions.

In Fig. 4, the significant wave height of the considered 14 load cases is plotted against the wind-wave misalignment. The area of the outer circles represents the load case probability of occurrence and the colored area corresponds to the percentage of the load case in which the TFA controller was active for total TFA activation time of 30 %. Fig. 4a and 4b illustrates the case without and with optimization, respectively. In the case without optimization, the proportion of the TFA activation time is same for all the sea states, here 30 %. In contrast, for the optimized case, TFA is activated only for a few load cases with extraordinary high loading. Therefore, instead of only switching the controller on and off to minimize the collateral effect, the 'smart' optimization approach described in Section 2.4 is beneficial.

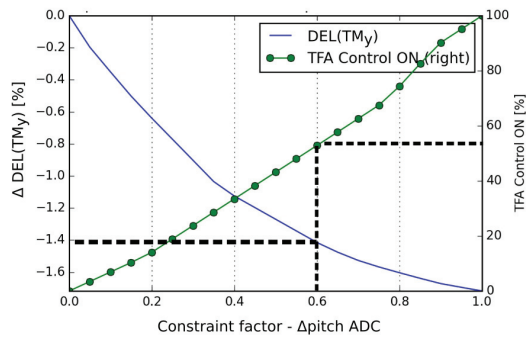


Fig. 5. Optimization for BLC and TFA with pitch ADC as constraint.

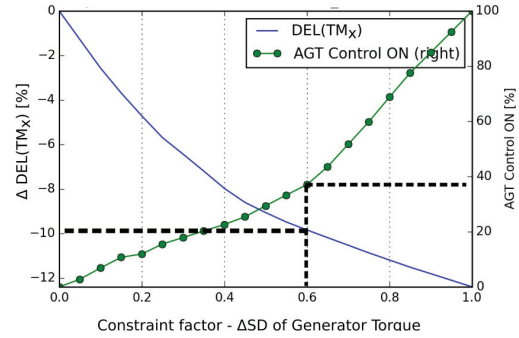


Fig. 6. Optimization for BLC and AGT with standard deviation of generator torque as constraint.

3. Results

3.1. Results of tailoring BLC versus TFA

The result of the multi-objective optimization performed to minimize the tower fore-aft damage equivalent load, $DEL(TM_y)$, limiting the pitch ADC is shown in Fig. 5. The primary y-axis represents the reduction on $DEL(TM_y)$ while the x-axis represents the different values for the constraint factor which gives the maximum allowable pitch ADC. The $DEL(TM_y)$ reduction is represented by a solid line and the corresponding percentage of TFA activation time by green line with markers. The decreasing slope of the $DEL(TM_y)$ line confirms that with a low limit of additional pitch ADC, the load cases with higher load reduction by relatively lower ADC penalty are chosen. For example, if the pitch ADC is allowed to increase to maximum 60 % of the total increase (shown with dashed line in Fig. 5), the $DEL(TM_y)$ will be reduced by 1.42 %, which corresponds to 82.4 % of the possible reduction when TFA is fully activated. In addition, TFA is activated for only 52.9 % of time. Furthermore, the additional pitch ADC increases almost linearly with TFA activation time (cf. linear slope of the activation curve) for the optimized load case selection. This demonstrates the opportunity to take advantage of the TFA controller to considerably reduce the TM_y load without overly increasing the pitch ADC. Hence, the trade-off analysis between the TFA and BLC could be performed successfully using the multi-objective optimization to minimize the fore-aft load and limiting the pitch ADC.

3.2. Results of tailoring BLC versus AGT

The result of the second multi-objective optimization which minimizes the tower side-to-side damage equivalent load ($DEL(TM_x)$) at mudline location, and limit the standard deviation of generator torque is plotted in Fig. 6. The reduced $DEL(TM_x)$ with respect to different values for the maximum allowable standard deviation of generator torque (constraint factors) is represented with the blue solid curve and the corresponding percentage activation time of AGT controller is shown with the green line with markers. In principle, the results look similar to the previously described fore-aft case. For example, if the standard deviation of the generator torque is allowed to increase to maximum 60 % of the possible increase (shown with dashed line in Fig. 6), the $DEL(TM_x)$ will be reduced by 9.8 %, which represents 70.4 % of the possible reduction if AGT was activated for 100 % of time. In addition, AGT is activated for only 37 % of time. However, here the characteristics of the dependency of the penalty effect on the activation time is less favourable than for TFA. The slope of the AGT activation time curve is increasing progressively with respect to the constraint factor. For instance activating AGT for 20 % of time results already in approximately 40 % of the overall increase in generator torque variability whereas activating TFA for the same duration results in approximately 25 % of the overall increase in pitch ADC (see Fig. 5). Nonetheless, the result confirms the possibility to take advantage of AGT controller to considerably reduce the TM_x load while limiting the extra standard deviation of generator torque.

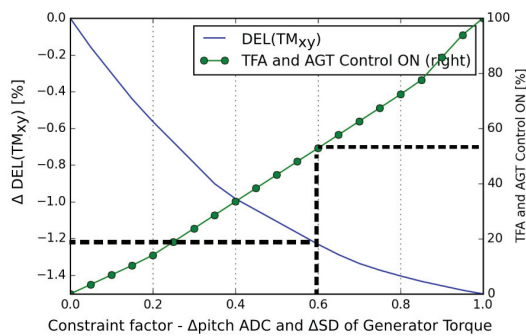


Fig. 7. Optimization for BLC, TFA and AGT with pitch ADC and standard deviation of generator torque as constraint.

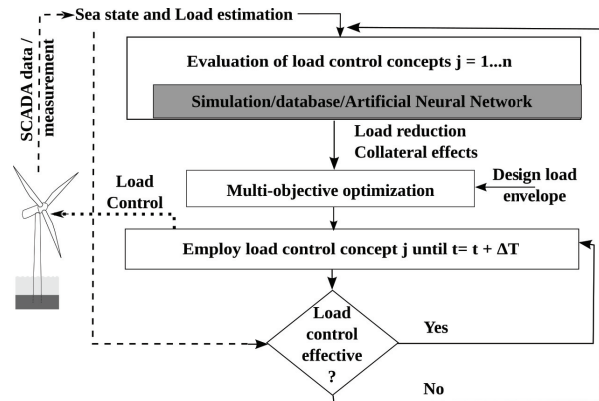


Fig. 8. Flowchart of the adaptive operational control.

3.3. Results of tailoring BLC versus TFA and AGT

Finally, Fig. 7 represents the results of the multi-objective optimization performed for three controllers. The reduced $\Delta \text{DEL}(\text{TM}_{xy})$ with respect to different values of the constraint factor for maximum allowable pitch ADC and standard deviation of generator torque is represented by the blue curve, and the corresponding percentage activation time of both TFA and AGT controller is shown by the green curve with markers. The plot looks very similar to the BLC versus TFA case in Fig. 5. For instance, if the constraint factor for the collateral effects is 0.6 (shown with dashed line in Fig. 7), the $\Delta \text{DEL}(\text{TM}_{xy})$ will be reduced by 1.2 %, which represents 82 % of the maximum achievable reduction. The corresponding reduction in fore-aft and side-to-side loads are 82.6 % and 55.6 % of the maximum achievable reduction when implementing TFA and AGT, respectively. The pitch ADC and standard deviation of generator torque are increased by 60 % and 51 % of the possible increase, respectively. The reduced $\Delta \text{DEL}(\text{TM}_{xy})$ of the superimposed tower fore-aft and side-to-side loads confirms that a trade-off analysis between the TFA, AGT and BLC controllers could be performed using the multi-objective optimization to minimize the resultant damage equivalent load while limiting both the pitch ADC and the standard deviation of generator torque.

4. Discussion

The multi-objective optimization approach presented in this paper and three optimization approaches demonstrated shows that the target load could be mitigated significantly while limiting the increase in the collateral effects. With the proposed optimization approaches, positive advantages offered by different available control concepts could be used while keeping the penalty within bounds. This is important because different controllers work most efficient at a certain operating range and are most suitable to reduce particular support structure loads [7]. The operating condition of the turbine is changing constantly over time, and therefore the operating range and the support structure loads vary. The selection of the controller in the trade-off analysis would depend on the sea state and the constraint factors used to limit the collateral effect in the multi-objective optimization. The constraint factor is selected according to the design limits of certain components and the lifetime of the turbine.

A more comprehensive system for adaptive operational control could be developed including this multi-objective optimization method. Fig. 8 illustrates such a possible adaptive operational control model. The selection of the most effective controller concept for a particular sea state condition and turbine load response would be facilitated by the multi-objective optimization. The optimization criteria depends on the reduced load and the collateral effect due to the implementation of one controller or the other for a particular load event and operating condition. This information will be available in a database or provided through an artificial neural network approach. The most effective controller concept chosen by the optimization will be activated for a certain length of time and both the sea state conditions

and the turbine load response would be constantly monitored online in order to decide if the implemented controller concept is still the most effective one.

However, to represent the load experienced by the support structure within its entire lifetime, the full operational wind speed range and sea state parameters as well as operational conditions should be considered. The load cases selected for the current paper are representative for the methodological approach only, but they are not sufficient to perform a full trade-off analysis. Moreover, there are optimization alternatives for the tailoring of BLC, TFA and AGT. One is to minimize the tower fore-aft and side-to-side loads instead of minimizing the superimposed load effect. For this purpose, different weighting is given to the loads depending on the sea state condition. Another approach is to minimize the maximum load on the monopile circumference.

5. Conclusion

This research introduced an approach for the trade-off analysis between the support structure load mitigation and collateral effects due to the situational employment of different controller concepts. It has been shown that the activation time of the controllers for each individual load case is selected by a multi-objective optimization approach, performing a trade-off analysis between different controllers. The optimization can select the most effective controller for each sea state to significantly reduce the target load, while limiting the collateral effects.

Acknowledgements

This work was partially funded by the German Federal Ministry for Economic Affairs and Energy (BMWi) in the scope of the RAVE (Research at Alpha Ventus) - OWEA Loads project (contract No. 0325577B). Acknowledgement is given to David Schlipf from the University of Stuttgart for providing the controller for the NREL 5MW turbine and other useful hints as well as to Adrian Jimenez for assisting in data handling and programming.

References

- [1] IRENA 2012. Renewable Energy Cost Analysis - Wind Power. IRENA Innovation and Technology Center. Germany; June 2012.
- [2] Staedler M. Controls for Load Reduction. In Proceedings of the Deutsche Windenergie Konferenz (DEWEK). Germany; 2008.
- [3] Bossanyi E. Wind Turbine Control for Load Reduction. Wind Energy. vol6:229-244. 2003. DOI: 10.1002/we.95.
- [4] van Engelen T, Schaak P, Lindenburg C. Control for Damping the Fatigue Relevant Deformation Modes of Offshore Wind Turbines. Presented at: 2003 European Wind Energy Conference - EWEA (ECN-RX03-037). Madrid, Spain; 2003.
- [5] Shan M, Jacobsen J, Adelt S. Field Testing and Practical Aspects of Load Reducing Pitch Control Systems for a 5 MW Offshore Wind Turbine. EWEA 2013, Scientific Proceedings; pp. 101-105. 2013.
- [6] Lackner M.A. An Investigation of Variable Power Collective Pitch Control for Load Mitigation of Floating Offshore Wind Turbines. Wind Energy. 2012. DOI: 10.1002/we.1502.
- [7] Fischer T. Mitigation of Aerodynamic and Hydrodynamic Induced Load of Offshore Wind Turbines. PhD Thesis. University of Stuttgart. Stuttgart, Germany; 2012.
- [8] Perrone F, Kuehn M. Offshore Wind Turbine Tower Fore-Aft Fatigue Load Reduction by Coupling Control and Vibrational Analysis. Journal of Ocean and Wind Energy (ISSN 2310-3604). Vol. 2, No. 3.; pp. 168175. August 2015. //dx.doi.org/10.17736/jowe.2015.mmr09.
- [9] Bossanyi E, Witcher D. UpWind - Controller for 5 MW reference turbine. UpWind Report 11593/BR/04. Garrad Hassan and Partners Limited. Bristol, England; July 2009.
- [10] Fischer T, de Vries W, Schmidt B. UpWind Design Basis WP4: Offshore Foundations and Support Structures. Stuttgart, Germany; 2010.
- [11] Kuehn M. Dynamics and design optimisation of offshore wind energy conversion systems. PhD Thesis. Delft University of Technology. Delft; 2001.
- [12] Bossanyi E. GH Bladed user manual. GL-Garrad Hassan. Bristol, England; 2010.
- [13] IEC 61400-3, Wind turbines - part 3: Design requirements for offshore wind turbines. International Electrotechnical Commission. Edition 1. Geneva; 2009.
- [14] Jonkman J, Butterfield S, Musial W, Scott G. Definition of a 5-MW reference wind turbine for offshore system development. NREL/TP-500-38060. National Renewable Energy Laboratory. USA; 2009.
- [15] Schlipf D. Lidar-assisted control concepts for wind turbines. Ph.D. Thesis. University of Stuttgart, in print, 2015.
- [16] Bottasso C L, Campagnolo F, Croce A, Tibaldi C. Optimization-Based Study of Bend-Twist Coupled Rotor Blades for Passive and Integrated Passive/Active Load Alleviation. Wind Energy. vol 16:1149-1166. 2013.
- [17] The Scipy community. Optimization and root finding. <http://docs.scipy.org/doc/scipy/reference/generated/scipy.optimize.linprog.html> (accessed 05.06.2016).